Copper Oxide ALD from a Cu(I) β-Diketonate: Detailed Growth Studies on SiO_2 and TaN

Thomas Waechtler [a] *, Nina Roth [b], Robert Mothes [b], Steffen Schulze [c], Stefan E. Schulz [a,d], Thomas Gessner [a,d], Heinrich Lang [b], and Michael Hietschold [c]

[a] Center for Microtechnologies (ZfM), [b] Department of Inorganic Chemistry, and [c] Solid Surfaces Analysis Group, Chemnitz University of Technology, D-09107 Chemnitz, Germany
[d] Fraunhofer Research Institution for Electronic Nano Systems (ENAS), D-09126 Chemnitz, Germany
*E-mail: thomas.waechtler@zfm.tu-chemnitz.de

The atomic layer deposition (ALD) of copper oxide films from [(^{n}Bu$_3$P)$_2$Cu(acac)] and wet oxygen on SiO_2 and TaN has been studied in detail by spectroscopic ellipsometry and atomic force microscopy. The results suggest island growth on SiO_2, along with a strong variation of the optical properties of the films in the early stages of the growth and signs of quantum confinement, typical for nanocrystals. In addition, differences both in growth behavior and film properties appear on dry and wet thermal SiO_2. Electron diffraction together with transmission electron microscopy shows that nanocrystalline Cu_2O with crystallites < 5 nm is formed, while upon prolonged electron irradiation the films decompose and metallic copper crystallites of ~ 10 nm precipitate. On TaN, the films grow in a linear, layer-by-layer manner, reproducing the initial substrate roughness. Saturated growth obtained at 120°C on TaN as well as dry and wet SiO_2 indicates well-established ALD growth regimes.

Introduction

Copper films with a thickness in the nanometer range are required as nucleation layers for the electrochemical Cu deposition to form multi-level interconnects in ultralarge-scale integrated (ULSI) electronic devices (1). Continuously shrinking device dimensions and increasing aspect ratios of the dual-damascene structures in the copper-based metallization schemes put ever more stringent requirements on the films with respect to their conformality in nanostructures and thickness homogeneity across large wafers. It appears therefore questionable if conventional physical vapor deposition (PVD) techniques will be able to meet those demands below the 32 nm technology node. Consequently, chemical gas-phase deposition methods such as chemical vapor deposition (CVD) or atomic layer deposition (ALD) are foreseen as potential alternatives to PVD (2). Due to its intrinsic self-limiting film growth characteristic, especially ALD appears appropriate for homogeneously coating complex substrates. However, depositing smooth and continuous metallic copper films by ALD has been found challenging, not only due to the strong agglomeration tendency Cu exhibits on many common substrate materials when subjected to heat. To overcome this issue, a copper oxide film may be grown by ALD under mild processing conditions, while a subsequent reduction step converts the copper oxide film to metallic copper. Apart from an application as starting point for Cu

nucleation layers, copper oxides (Cu_2O, CuO) appear interesting also for other reasons. Being semiconductors and available in abundant quantities, they are of potential interest for future low-cost photovoltaic applications (3). In addition, Cu_2O and CuO exhibit a number of interesting properties, for example, with respect to their catalytic behavior (4, 5) and gas-sensing properties (6, 7). We are therefore interested in studying ALD processes for the growth of copper oxide films from Cu(I) β-diketonate precursors. Based on earlier communications concerning the ALD on Ta, TaN, Ru, and SiO_2 (8, 9), we here report detailed film growth studies in the self-limiting regime on SiO_2 and TaN. The optical properties of the copper oxide films grown on SiO_2 will be discussed as well.

Experimental

Copper oxide films were grown from the copper(I) β-diketonate precursor [(^{n}Bu$_3$P)$_2$Cu(acac)] (Bu = butyl) and wet oxygen in similar processes as described in Ref. 9. In the course of those studies, temperature-independent growth was found between 110 and 125°C on SiO_2 and TaN.

Prior to ALD, 100 mm Si wafer substrates were thermally oxidized in a Centrotherm tube furnace. For the experiments, two types of thermal SiO_2 were fabricated: Thin silica films of 20 nm thickness were obtained by dry oxidation at 900°C by flowing 6000 sccm O_2 together with 100 sccm HCl gas to getter metallic contaminants. Thicker SiO_2 films of 300 nm were grown by wet oxidation at 1000°C from in-situ burning of H_2 with O_2 in a flow ratio of 13:8 for 30 min and 18:6 for the remaining 14 min of the process. TaN underlayers of 40 nm thickness were deposited by reactive sputtering in a Balzers CLC 9000 tool (10).

Immediately after the ALD, ex-situ spectroscopic ellipsometry was used for characterization of the samples. The investigations were carried out on a SENTECH SE 850 ellipsometer, typically at incidence angles of 50, 60, and 70° in the spectral range from 190 to 830 nm. The ellipsometric data were processed using the software SpectraRay 2, available with the SE 850. To separate the properties of the ALD layers from the respective substrates, the 20 nm and 300 nm SiO_2 films as well as the 40 nm TaN films were studied by ellipsometry prior to the ALD processes so that adequate substrate models could be generated. To describe the Si substrates as well as the SiO_2 films, models available in the database of SpectraRay 2 were applied and modified to some extent, in order to account for different optical properties of the thin and thick SiO_2 layers. To describe the properties of the TaN films, Lorentz-Drude models, as discussed earlier (10, 11), were used.

To investigate the surface morphology of the ALD films, atomic force microscopy (AFM) was carried out using a Digital Instruments NanoScope IIIa AFM with standard silicon tips in tapping mode. Selected samples were further investigated with transmission electron microscopy (TEM) and electron diffraction, using a Philips CM 20 TEM equipped with a field-emission gun.

Results and Discussion

ALD on SiO_2

Films grown both on 20 nm dry and 300 nm wet thermal silicon oxide were ellipsometrically characterized by modeling their dielectric function with a Lorentz-Drude approach (12). Fig. 1 presents spectra of the measured ellipsometric parameters Ψ

and Δ and the fitted curves for a representative sample, applying four oscillators. For the Lorentz-Drude model, SpectraRay 2 uses the representation according to equation [1] and gives the oscillator parameters in units of cm^{-1} of the wave number ν.

$$\tilde{\varepsilon}(\nu) = \varepsilon_\infty + \frac{\omega_p^2}{-\nu^2 - i\,\omega_\tau\,\nu} + \sum_{k=1}^{n} \frac{\Omega_{pk}^2}{\Omega_{0k}^2 - \nu^2 - i\,\Omega_{\tau k}\,\nu} \qquad [1]$$

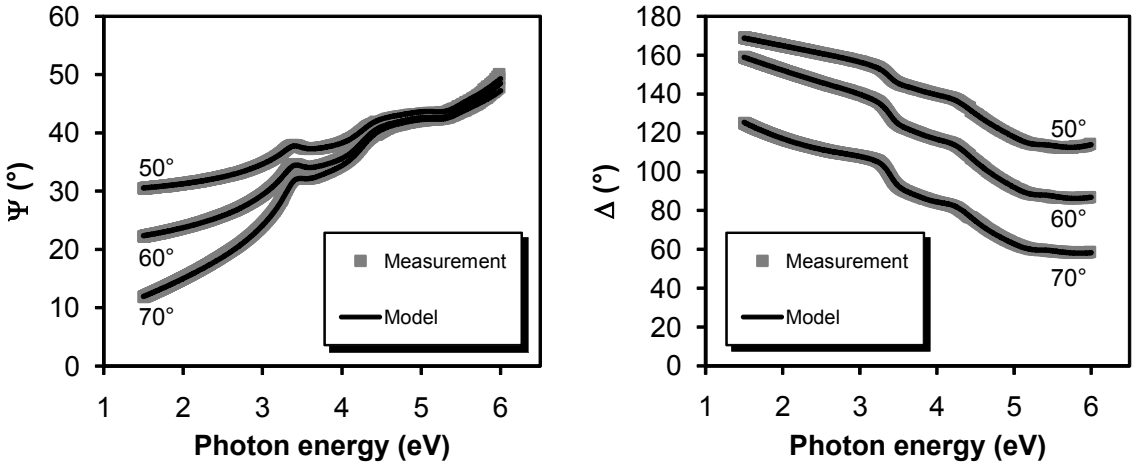

Figure 1. Measured and modeled spectra of Ψ (left) and Δ (right) for a 5.4 nm copper oxide film grown on 20 nm dry SiO_2.

Equation [1] thereby describes the complex dielectric function $\tilde{\varepsilon}(\nu) = \varepsilon_1 + i\varepsilon_2$ as a superposition of a high-frequency contribution ε_∞, a Drude term to account for free carriers, and a certain number of Lorentzian oscillators. Each of them is characterized by an oscillator strength Ω_p, a center frequency Ω_0, and a damping constant Ω_τ. The Drude term, as a quasi-oscillator at zero center frequency, contributes another two model parameters: the plasma frequency ω_p and a damping parameter ω_τ. In the ellipsometric models, roughness effects were not introduced for two reasons. Because substrate roughness was below 2 Å in case of the SiO_2 substrates and smaller than 4 Å on TaN, it could be neglected. The ALD films were also considered as homogeneous layers, because introducing effective medium models to account for rough films or inhomogeneities offer additional degrees of freedom in the models. On the one hand, those could improve the fitting results. On the other hand, such approaches can also lead to uncertainties from a practical point of view, for example with respect to the ratio of the materials forming the effective medium, any gradients that may be present in the film, and even the physical thickness of the layer.

In this respect, Table I lists the parameters of the oscillator model used for the fit presented in Fig. 1, converted to the eV scale. As can be seen, the parameters of the Drude term are set to zero. During the fitting routine it was repeatedly found that adding this term would lead to considerable correlation among the parameters, making the models unreliable. Apparently in the spectral range studied a contribution to the dielectric function from free carriers is not relevant. Since we found from XPS that the ALD films mainly consist of Cu_2O and some CuO or $Cu(OH)_2$ toward the surface (9), it also appears reasonable that no Drude term is required. For verification, selected samples were studied

by transmission electron microscopy (TEM) and electron diffraction. Fig. 2 a shows a lateral TEM image of an ALD film grown on 20 nm SiO_2, indicating a nanocrystalline structure with crystallites of below 5 nm size. The corresponding electron diffraction result in Fig. 2 b perfectly matches the pattern to be expected for cuprite, i.e., Cu_2O.

TABLE I. Parameters of the Lorentz-Drude model used for fitting the (Ψ, Δ) spectra shown in Fig. 1 (4 oscillators).

Film thickness (nm)	ε_∞	ω_p (eV)	ω_τ (eV)	Ω_{0k} (eV)	Ω_{pk} (eV)	$\Omega_{\tau k}$ (eV)
5.4	2.81	0.0	0.0	4.52	2.88	1.24
				5.45	4.25	1.64
				3.72	3.60	2.08
				2.95	2.36	1.06

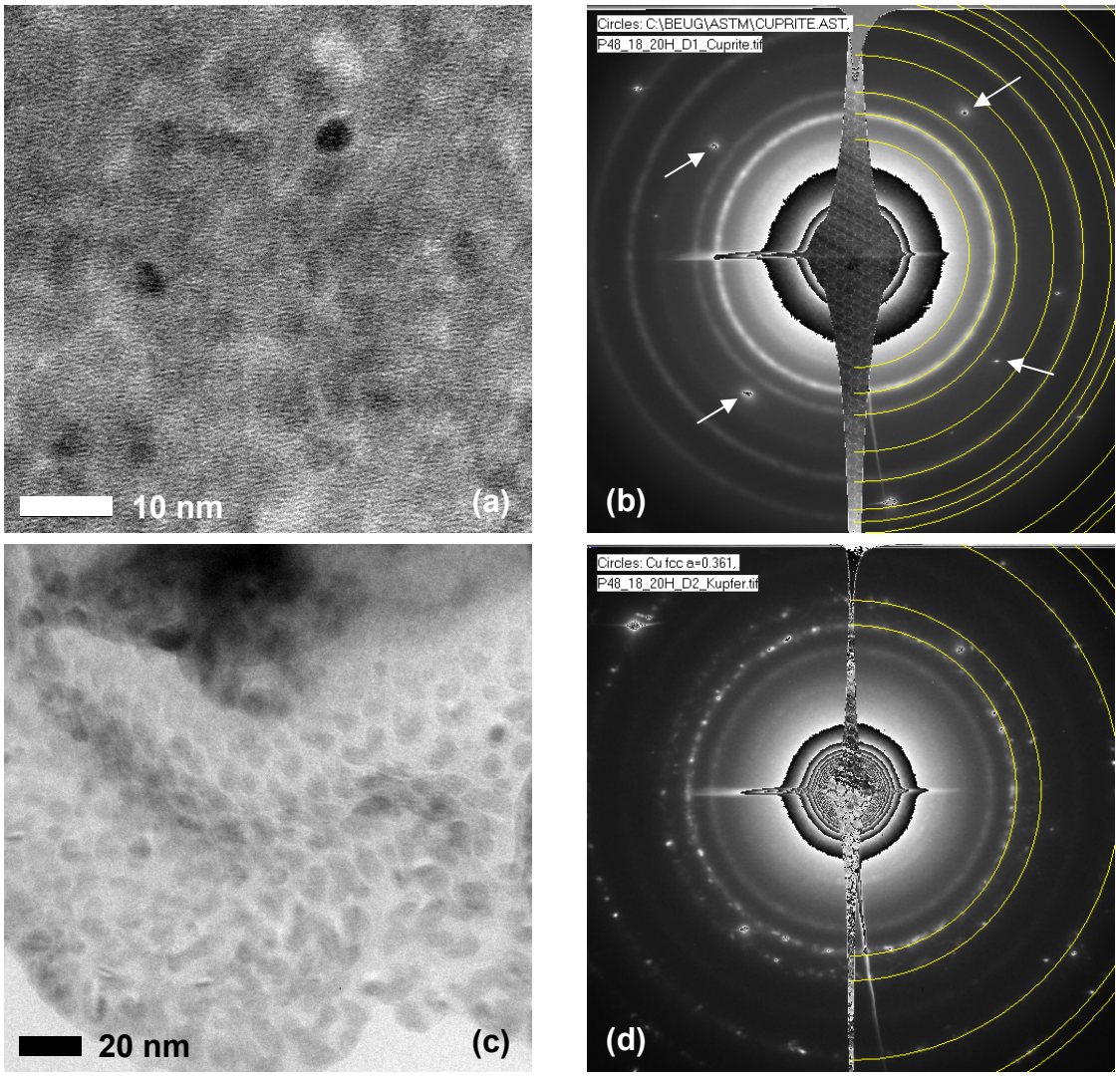

Figure 2. Plan-view TEM image (a) of a ~ 5 nm ALD film grown on 20 nm SiO_2. The film appears nanocrystalline with crystallites of < 5 nm. Electron diffraction (b) reveals that the film consists of Cu_2O. The diffraction pattern perfectly matches the one expected for cuprite. Reflexes marked with arrows in this image stem from the single-crystalline Si (100) substrate. After prolonged electron beam irradiation, crystallites of ~ 10 nm began to form (c). Those were identified as metallic Cu, indicated by the semicircles overlaid the diffraction pattern in image (d).

After prolonged exposure of the sample to the electron beam, larger crystallites of ~ 10 nm began to form in the film. By electron diffraction, those were identified as metallic Cu. Similar effects were also observed during X-ray photoelectron spectroscopy (XPS) when recording Ar ion-sputtered depth profiles. With increasing sputtering depth, the ALD films changed from oxidic to metallic copper, contradictory to the data obtained from angle-resolved XPS. This suggests that the copper oxide films undergo decomposition upon prolonged irradiation with electrons or ions.

The plot of the film thickness derived from the ellipsometric measurements as a function of the number of ALD cycles (Fig. 3 a) shows a behavior that could be attributed to island growth in conjunction with substrate enhancement effects: During the first cycles, a rather steep, nonlinear increase in film thickness is seen, whereas, as the islands coalesce with increasing number of ALD cycles, the curve flattens toward a linear characteristic with a constant growth-per-cycle (GPC) (13, 14). In fact, AFM investigations reveal that during the initial stages of the ALD process the smooth surface of the flat SiO_2 films considerably roughens before it again becomes smoother as a consequence of the formation of a continuous film, which has been shown theoretically to be typical for island growth (14). In this respect, Fig. 4 shows respective AFM results, while Fig. 5 depicts the evolution of the surface roughness, calculated from the AFM data. For ALD samples grown during 400 cycles, the data suggest only a minor influence of the precursor pulse length on the roughness of the films. In fact, very good saturation of the GPC for precursor pulses longer than 2 s was obtained (Fig. 3 b). However, there appears to be a difference in the growth behavior on the dry 20 nm SiO_2 compared to the thicker SiO_2 films grown by wet thermal oxidation.

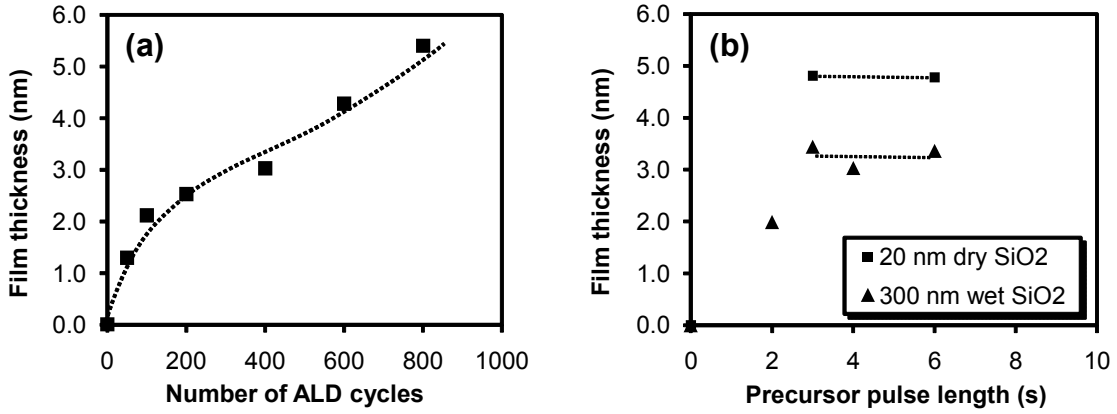

Figure 3. (a) ALD film thickness as a function of the number of cycles for the growth on 300 nm SiO_2. (b) Resulting film thickness after 400 ALD cycles with varying precursor pulse length suggesting saturated growth at 120°C as well as differences in the growth behavior on SiO_2 formed by dry or wet thermal oxidation.

The dielectric functions of the copper oxide films extracted from the ellipsometric models also suggest a substrate influence on the properties of the films. As seen from the data measured for ALD films on 20 nm SiO_2 (Fig. 6 a and b), the dielectric function strongly varies during the initial stages of the ALD. This is attributed to the island-growth behavior and could be related to quantum-confinement effects known for semiconductor nanoparticles (15). With increasing number of ALD cycles, the dielectric functions tend to saturate. However, the characteristics of ε_2 suggest band gaps above 2 eV also for the thicker films, while for bulk Cu_2O a band gap energy of ~ 2 eV is typical (16). Taking

into account the TEM results, which indicate nanocrystalline films to be present still after 800 cycles, band gap energies of > 2 eV would be in line with data reported for nanocrystalline Cu_2O prepared by other methods (17, 18). In contrast to the results on 20 nm dry thermal SiO_2, the dielectric function for Cu_2O films on thicker SiO_2 grown by wet oxidation appears remarkably blue-shifted (Fig. 6 c and d). However, although these data were repeatedly obtained from the Lorentz-Drude models for the copper oxide films, one still might question the results at this stage as the spectra of ε_2 suggest band gap energies well above 3 eV. Therefore, additional studies, such as ALD on wet-grown SiO_2 films of different thickness as well as alternative modeling approaches or different optical characterization methods, need to be carried out for verification. Nevertheless, the results suggest that slightly altering the substrate properties could considerably influence the ALD growth as well as the resulting film properties.

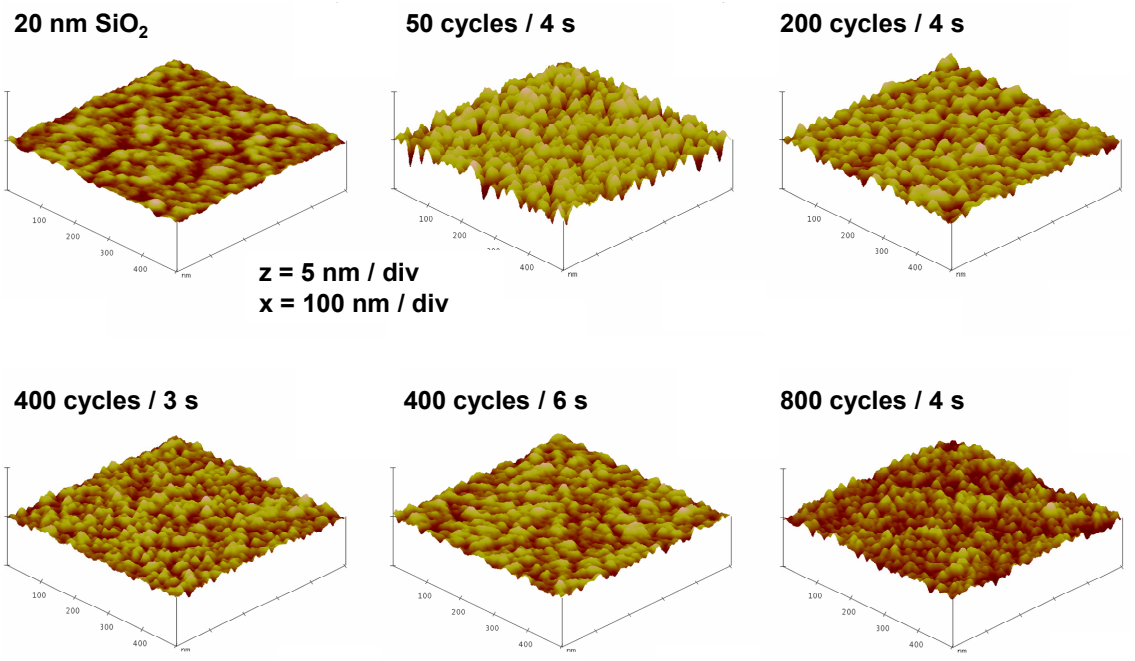

Figure 4. Surface morphology of an initial 20 nm SiO_2 film as well as after ALD processes with varying number of cycles. While the processes with 50, 200, and 800 cycles were carried out with precursor pulses of 4 s, the pulse length was varied between 3 and 6 s for processes of 400 cycles.

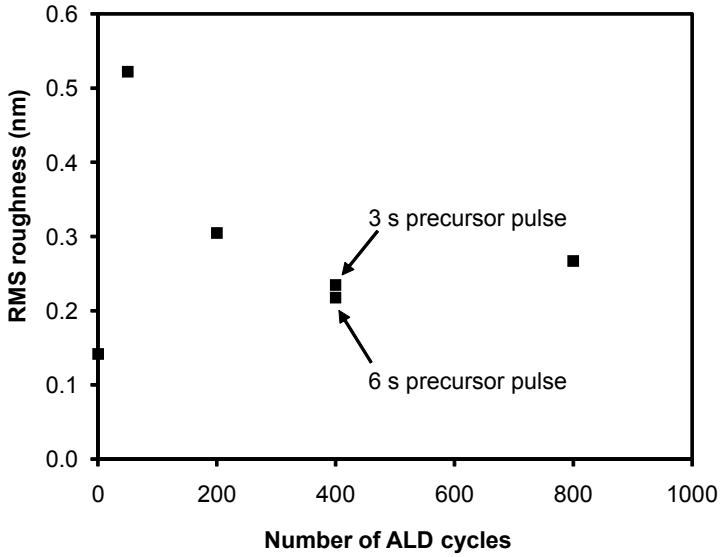

Figure 5. Evolution of surface roughness with increasing number of ALD cycles during growth on 20 nm SiO_2. The values of the root mean square (RMS) roughness were calculated from AFM data. If not otherwise noted, the processes were carried out with precursor pulses of 4 s.

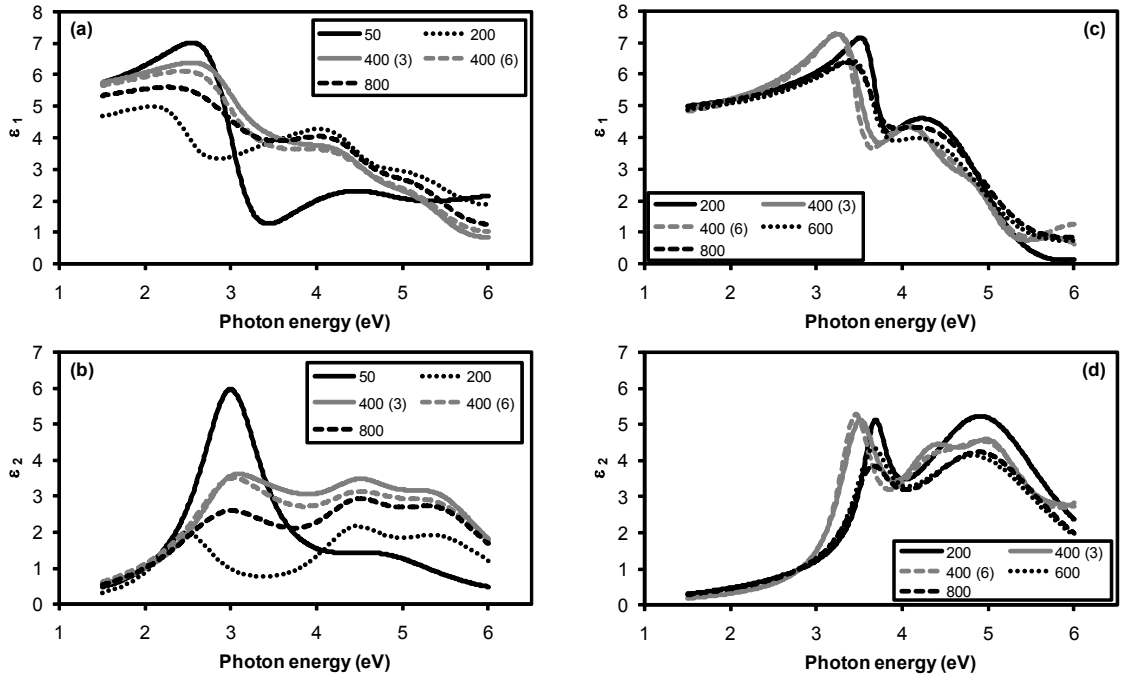

Figure 6. Complex dielectric function of ALD-grown copper oxide films extracted from ellipsometric modeling. (a) and (b) represent results obtained for films grown on 20 nm dry SiO_2, while (c) and (d) display the properties of ALD films deposited on 300 nm wet thermal SiO_2. The processes were carried out with 50 to 800 ALD cycles and 4 s precursor pulses, except for the experiments with 400 cycles. For those, data obtained from films grown with 3 and 6 s precursor pulses are shown.

ALD on TaN

To deposit seed layers required for electrochemical copper deposition in metallization schemes of ULSI devices, the ALD on refractory metal-based diffusion barrier materials is of particular interest. For detailed characterization of the copper oxide ALD from [(^{n}Bu$_3$P)$_2$Cu(acac)] and wet oxygen on TaN, processes were therefore carried out at 120°C, essentially in the ALD window established previously (9). Processes of 400 cycles with varying precursor pulse length displayed good saturation of the GPC, indicating a well-established ALD growth (Fig. 7 a). Furthermore, as seen from Fig. 7 b, the films grow in a linear manner with increasing number of ALD cycles. In contrast to the island growth observed on SiO_2, this indicates layer-by-layer growth on TaN. These findings, which are derived from the film thickness values obtained from spectroscopic ellipsometry, are supported by AFM investigations. In this respect, Fig. 8 displays images of the surface morphology at different stages of the film growth. Fig. 9, showing the film roughness as a function of the number of ALD cycles, complements this investigation. Evidently, there is no clear trend in the evolution of the roughness. The initial roughness of the TaN substrate is largely reproduced by the ALD film, while a slight variation of the morphology with the precursor pulse length is seen. Together with the AFM images this also points to the two-dimensional growth on TaN. This result needs to be stressed especially when considering the fact that Cu is very susceptible to the formation of islands and agglomeration on transition metals and their nitrides. Nevertheless, ultra-thin, continuous copper films on such substrates are highly desirable for nanoscale interconnect structures. Because especially thermal ALD is generally capable of producing conformal films in demanding three-dimensional nanostructures, a process to deposit continuous, copper oxide films could be a viable basis for the formation of thin Cu seed layers.

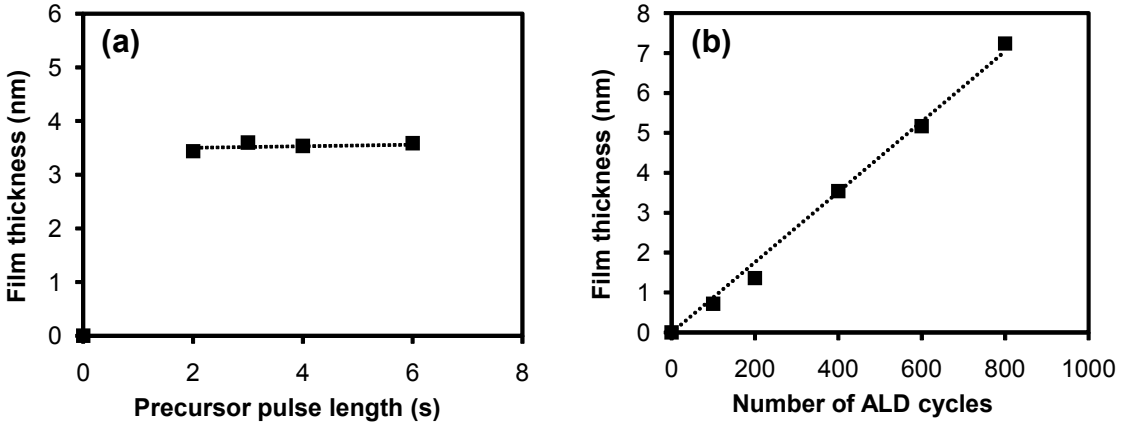

Figure 7. (a) Resulting film thickness on TaN after ALD processes with 400 cycles and varying precursor pulse length. The saturating behavior indicates well-established ALD growth. (b) Film thickness derived from spectroscopic ellipsometry as a function of the number of ALD cycles, indicating linear growth on TaN.

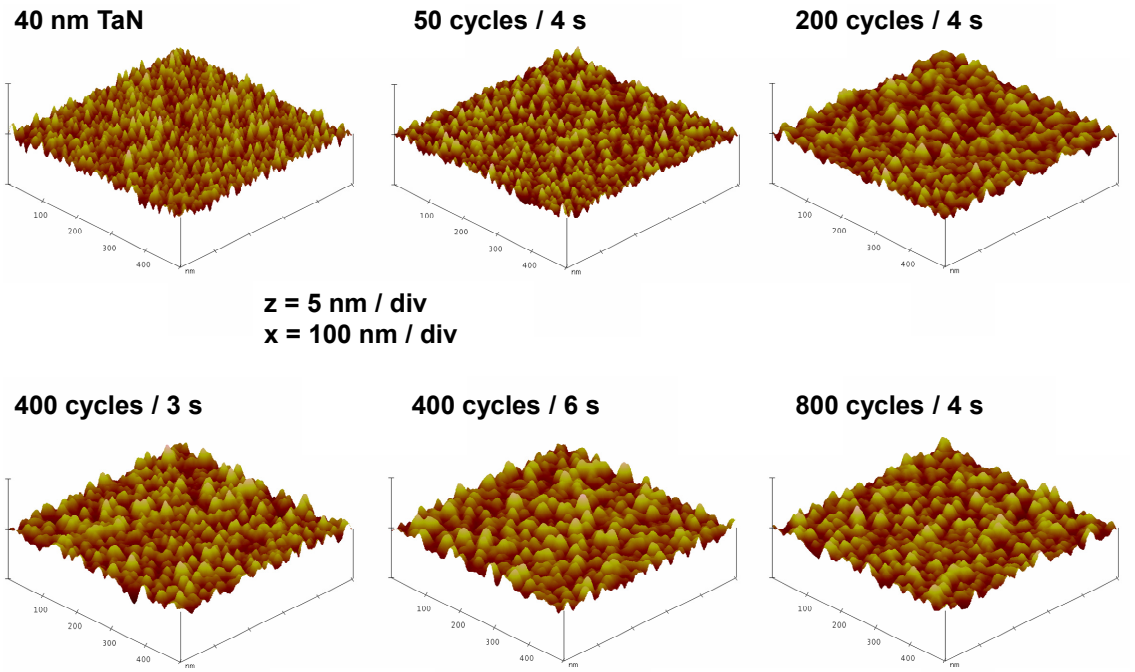

Figure 8. Surface morphology of an initial 40 nm TaN film as well as after ALD processes with varying number of cycles. While the processes with 50, 200, and 800 cycles were carried out with precursor pulses of 4 s, the pulse length was varied between 3 and 6 s for processes of 400 cycles.

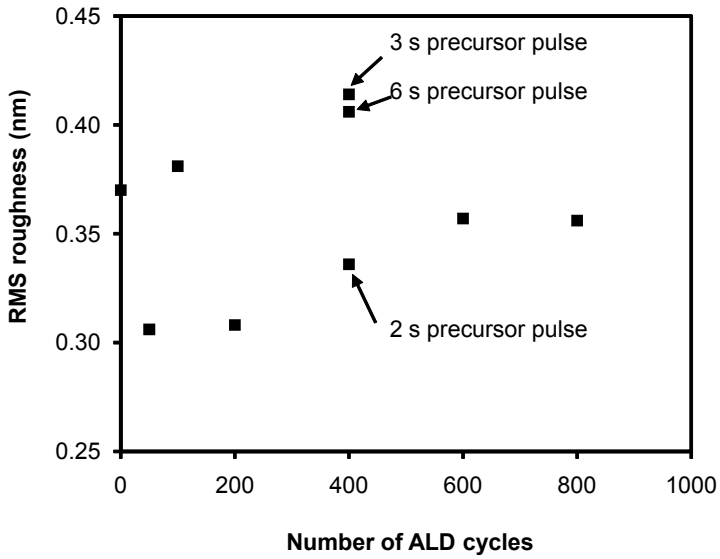

Figure 9. Evolution of surface roughness with increasing number of ALD cycles during growth on 40 nm TaN. If not otherwise noted, the processes were carried out with precursor pulses of 4 s.

Summary

Due to their properties, copper oxides and especially Cu_2O appear interesting for a number of applications. These include their potential relevance for use in cost-effective photovoltaic devices as well as a starting point for ultra-thin copper seed layers to fabricate the complex multilevel metallization scheme in ULSI devices. In the latter case, films need to be deposited on materials such as TaN, a typical Cu diffusion barrier, and must be smooth and continuous already at thicknesses of only several nanometers.

We have shown that by using $[(^{n}Bu_3P)_2Cu(acac)]$ and wet oxygen as precursors in thermal ALD, continuous films with comparable roughness as the initial substrate can be deposited on TaN at temperatures as low as 120°C in a linear growth regime without signs of agglomeration. Saturated growth was also obtained on SiO_2 substrates. However, the ALD films here exhibit island growth behavior. This is expressed both in a non-linear film thickness characteristic up to ~ 200 ALD cycles as well as in a strong variation of the dielectric function of the films in this range, pointing to quantum confinement effects typically observed for nanocrystalline materials. Furthermore, a considerable variation of both the GPC and the optical properties was observed for films grown either on dry or wet thermal silicon oxide. However, as varying optical properties with film thickness in the low nanometer range can create uncertainties in modeling the ellipsometric data especially with respect to the optical function, these results need to be further verified. Nevertheless, the studies indicate that both film growth and properties can potentially be tuned by even slight variations of the substrate.

For a later application of the films as seed layers in electroplating to form interconnects, the copper oxide obtained from ALD needs to be reduced. Results obtained so far indicate this to be challenging for films grown on TaN with pure thermal reduction processes only. In contrast, good results have been obtained with low-temperature thermal reduction using organic reducing agents for copper oxide films grown on ruthenium. An in-depth study of the ALD growth, copper oxide reduction, and an application of those films grown on Ru in copper electroplating will be reported separately.

Acknowledgments

Financial support from the German Research Foundation (DFG) in the International Research Training Group 1215 “Materials and Concepts for Advanced Interconnects” and the “Fonds der Chemischen Industrie” is gratefully acknowledged. We further thank Dr. B. Gruska (SENTECH Instruments) as well as S. Hermann (Center for Microtechnologies) for helpful discussions, and acknowledge R. Müller and N. Zichner (Center for Microtechnologies) for technical assistance.

References

1. K. Weiss, S. Riedel, S. E. Schulz, M. Schwerd, H. Helneder, H. Wendt, and T. Gessner, *Microelectron. Eng.,* **50,** 433 (2000).
2. *ITRS – The International Technology Roadmap for Semiconductors, 2007 Ed.,* European Semiconductor Industry Association, Japan Electronics and Information Technology Industries Association, Korean Semiconductor Industry Association, Taiwan Semiconductor Industry Association, and United States Semiconductor Industry Association, Editors, available at http://www.itrs.net/reports.html (2007).

3. C. Wadia, A. P. Alivisatos, and D. M. Kammen, *Environ. Sci. Technol.,* **43**, 2072 (2009).
4. J. Ramírez-Ortiz, T. Orgura, J. Medina-Valtierra, S. E. Acosta-Ortiz, P. Bosch, J. A. de los Reyes, and V. H. Lara, *Appl. Surf. Sci.,* **174,** 177 (2001).
5. T. Ben-Moshe, I. Dror, and B. Berkowitz, *Appl. Catal. B,* **85,** 207 (2009).
6. S. T. Shishiyanu, T. S. Shishiyanu, and O. I. Lupan, *Sens. Actuators B,* **113,** 468 (2006).
7. Y. Zhang, X. He, J. Li, H. Zhang, and X. Gao, *Sens. Actuators B,* **128,** 293 (2007).
8. T. Waechtler, S. Oswald, A. Pohlers, S. Schulze, S. E. Schulz, and T. Gessner, in *Conference Proceedings AMC XXIII, Advanced Metallization Conference 2007*, A. J. McKerrow, Y. Shacham-Diamand, S. Shingubara, and Y. Shimogaki, Editors, p. 23, Materials Research Society, Warrendale, PA (2008).
9. T. Waechtler, S. Oswald, N. Roth, A. Jakob, H. Lang, R. Ecke, S. E. Schulz, T. Gessner, A. Moskvinova, S. Schulze, and M. Hietschold, *J. Electrochem. Soc.,* **156,** H453 (2009).
10. T. Waechtler, B. Gruska, S. Zimmermann, S. E. Schulz, and T. Gessner, in *Conference Proceedings 8th International Conference on Solid-State and Integrated Circuit Technology (ICSICT 2006),* p. 2184 (2006).
11. S. Rudra, T. Wächtler, M. Friedrich, S. J. Louis, C. Himcinschi, S. Zimmermann, S. E. Schulz, S. Silaghi, C. Cobet, N. Esser, T. Gessner, and D. R. T. Zahn, *phys. stat. sol. (a),* **205,** 922 (2008).
12. H. G. Tompkins and W. A. McGahan, *Spectroscopic Ellipsometry and Reflectometry. A User's Guide,* p. 26, John Wiley & Sons, Inc., New York (1999).
13. R. L. Puurunen and W. Vandervorst, *J. Appl. Phys.,* **96,** 7686 (2004).
14. O. Nilsen, O. B. Karlsen, A. Kjekshus, and H. Fjellvåg, *Thin Solid Films,* **515,** 4527 (2007).
15. L. Brus, *Appl. Phys. A,* **53,** 465 (1991).
16. R. J. Elliott, *Phys. Rev.,* **124,** 340 (1961).
17. K. E. R. Brown and K.-S. Choi, *Chem. Commun.,* 3311 (2006).
18. K. Borgohain, N. Murase, and S. Mahamuni, *J. Appl. Phys.,* **92,** 1292 (2002).